K x-ray production in single collisions of chlorine and sulfur ions*

Loren Winters,† Matt D. Brown, Louis D. Ellsworth, Tang Chiao,‡ E. W. Pettus,§ and James R. Macdonald
Department of Physics, Kansas State University, Manhattan, Kansas 66506
(Received 26 August 1974)

Cl K x-ray-production cross sections have been measured in single collisions of 0.1–1.5-MeV/amu Cl ions with gas targets of He, N_2, Ne, SiH_4, H_2S, HCl, Ar, Kr, and Xe. Cross sections for Ne K, Si K, S K, Ar K, Kr L, and Xe L x-ray production and yields for Xe M x rays were also obtained. Similar measurements for both Cl and S ions were made at one velocity as a function of projectile charge state q for $5 \leq q \leq 11$. Except at the highest energies, projectile K x-ray-production cross sections are nonmonotonic as a function of target atomic number Z_2. Anomalously high target and projectile cross sections occur in the symmetric region: $Z_2 \simeq 17$. For all x-ray lines, the cross sections show an increase with increasing q at constant projectile velocity, with the rate of increase being greatest in the symmetric region. The experimental results indicate the importance of one-step molecular processes suggested by Meyerhof in producing K vacancies. The $2p\sigma$-$2p\pi$ transition may be of importance when initial $2p$ vacancies are carried into K-vacancy-producing collisions. The large cross sections for both target and projectile in nearly symmetric collisions gives evidence for K-vacancy transfer between collision partners.

I. INTRODUCTION

Numerous experimental investigations[1] of ion-atom collisions in the past 20 years have established the importance of Coulomb ionization and electron promotion[2] for the production of inner-shell vacancies. Theoretical studies[2-5] of these interactions are supported by the experimental observations for certain ranges of the parameters Z_1/Z_2 and v/v_0, where Z_1 and Z_2 are projectile and target nuclear charges, respectively, v is the projectile velocity, and v_0 is the mean velocity of the target electron. For light ions (protons, deuterons, alpha particles) incident on heavy targets ($Z_1/Z_2 \ll 1$) and with Coulomb deflection and polarization effects[6] taken into account, a Coulomb-ionization calculation[3] has been shown to account for the target inner-shell-vacancy production over a velocity range extending from $v/v_0 \ll 1$ to $v/v_0 \gtrsim 1$.

For heavier projectiles (but Z_1/Z_2 still less than unity) at intermediate velocities ($v/v_0 \gtrsim 1$), experimental[7,8] and theoretical[9] investigations give evidence that K-electron transfer to bound states of the projectile is increasingly important to K-vacancy production. For fully stripped projectiles in particular, this mechanism may be dominant. At higher velocities ($v/v_0 > 1$), recent experimental results[10] suggest that charge transfer is not important in K-vacancy production and that Coulomb ionization again dominates.

The emphasis of the experiment presented in this paper is on the symmetric collision region $Z_1 \simeq Z_2$, as compared to the asymmetric regions $Z_1/Z_2 < 1$ and $Z_1/Z_2 > 1$. Quantitative studies of rotational-coupling-induced transitions between transient molecular orbitals in symmetric collisions[11] have had reasonable success in explaining experimental results in the adiabatic region ($v/v_0 \ll 1$). Nonmonotonic behavior of Ar L x-ray-production cross sections as a function of target or projectile atomic number[12] have been qualitatively understood in terms of energy-level matching and the molecular model.[2,5] At the intermediate velocities studied in this paper, however, little is understood about the details of K-vacancy production. Coulomb ionization and excitation, electron promotion, and electron transfer may all have important influences on the vacancy production. Experimental studies of bromine and nickel x-ray production by Kubo *et al.*[13] and chlorine radiation by Woods *et al.*[14] have been used to suggest that the $2p\sigma$-$2p\pi$ molecular-orbital transition induced by rotational coupling of these orbitals may account for the relatively high K x-ray-production cross sections for nearly symmetric systems. This transition requires initial $2p$ vacancies which may be produced by prior collisions in the thick targets that were used in those experiments.

In a previous publication,[15] we have shown that the cross sections for Cl K x-ray production in the nearly symmetric Cl-Ar collision at 5–52 MeV are anomalously high in comparison to asymmetric collisions involving Cl projectiles. Since these measurements were carried out with thin, gas targets that approximate single-collision conditions for electron loss by projectiles with no initial $2p$ vacancies, the $2p\sigma$-$2p\pi$ transition can only explain the experimental results if the $2p$ excitation cross sections are very large. Meyerhof[16] has proposed that excitation of $2p\sigma$ electrons to continuum states may explain the experimental

results. Experimental knowledge of the validity of these suggestions is essential to an understanding of K-vacancy production in symmetric collisions.

Toward this end, we have undertaken a more detailed study of these collisions. Preliminary results of this study have previously been reported.[17] For equal velocity Cl and S projectiles, we have measured target and projectile absolute x-ray-production cross sections as a function of projectile charge state q for $5 \leq q \leq 11$. Thin, gas targets of Ne, SiH_4, H_2S, HCl, Ar, HBr, Kr, and Xe were used. The range of charge states used allows one to determine the effect of initial $2p$ vacancies in the Cl and S ions on the x-ray production. Our results suggest that the $2p\sigma$ -$2p\pi$ transition is of importance to K-vacancy production when initial projectile $2p$ vacancies are brought into the K-vacancy-producing collisions. However, if these initial $2p$ vacancies are not present, a single-step molecular process such as that proposed by Meyerhof[16] may be dominant. Moreover, the possibility of K-vacancy sharing[18] by target and projectile is indicated.

II. EXPERIMENTAL APPARATUS AND METHODS

The KSU tandem Van de Graaff accelerator was used to directly accelerate chlorine beams in charge states +2 to +8 over an energy range of 3.0 to 52.2 MeV. The beams were momentum-analyzed by a 90° bending magnet. A thin carbon foil was placed between the analyzing and switching magnets to obtain a distribution of charge states of chlorine and sulfur beams at the same velocity. For some of the charge states, the direct beam was used in lieu of the post-stripped beam in order to obtain greater intensity, and in all cases the beam velocity was kept constant by slight adjustments of the field of the analyzing magnet.

Beams of each charge state were selected separately by the switching magnet and were passed through the differentially pumped gas target chamber. The chamber, the beam collimation, and the current-normalization procedure were described in a previous publication.[8] The pressure in the beam tube was typically 10^{-7} Torr, and the residual pressure in the gas cell was approximately 10^{-5} Torr. Charge-state analysis[19] of beams emerging from the gas cell indicated that the incident charge-state purity was always better than 98%. Beam currents of several nanoamperes were typical for most charge states but in some cases were as low as tenths of nanoamperes. An effective low-current limit of the Brookhaven integrator used was approximately 0.05 nA, for which zero drift of the electronic circuitry introduced an uncertainty of about 10% in x-ray yields normalized to the integrator output.

Target pressure was determined by a capacitance manometer. Details of the gas-handling system have been described in an earlier publication.[20] X-ray yields were measured at pressures of 1 to 10 m-Torr with a gas-cell length of 5.5 cm. The growth of x-ray yield with pressure was linear in this range, as well as to considerably higher pressures. For each x-ray peak with each projectile charge state and velocity, x-ray yields were measured for at least two and usually as many as five pressures.

Two Si(Li) detector systems were used to detect x rays produced in the gas cell. Both detectors had similar specifications for crystal location and size (80 $mm^2 \times 3$ mm) and beryllium-window thickness (0.025 mm). At 6 keV, the resolution was typically 200 and 250 eV for detectors A and B, respectively. The tailing behavior[20] of detector A (supplied by KeVex Corp.) was severe (see Sec. III), presumably owing to incomplete charge collection with the low detector bias (500 V) used. Although system B[21] had somewhat poorer resolution than A, it had the advantages of almost negligible tailing effects and almost no amplifier dead time such as that present for the pulsed optical feedback system of detector A with the threshold set low to optimize resolution. Energy calibration was by an ^{55}Fe source as well as by proton-induced excitation of gas targets.

For the geometrical factors used to obtain cross sections, x rays were assumed to be emitted isotropically. Two graphite sleeves served to define the interaction region seen by the detectors and shield them from the gas-cell apertures. Recent experimental results[22] indicate that the emission of FK x rays in 33-MeV-F^{+9}–on–Ar collisions is somewhat anisotropic, the probability of x-ray emission being greatest at 90° to the beam direction. If such anisotropy exists for the x-ray emission by Cl and S ions with $5 \leq q \leq 11$, the reported cross sections will be systematically high. However, the interpretations of the data are not expected to change.

An important consideration in these experiments is the probability for multiple collisions. Although single-collision conditions with respect to K-vacancy production were maintained throughout the experiment, the linear growth of K x-ray yield with pressure does not ensure that collisions involving charge exchange or excitation do not occur with sufficient probability to affect the x-ray yields. To estimate the magnitude of these effects, charge-exchange cross sections for chlor-

ine ions were measured in a separate experiment.[19] Although the cross sections are different for all the cases studied in this experiment, for the worst case (18-MeV Cl-Ar) approximately 20% of the beam undergoes single charge exchange of outer-shell electrons in the target. This is estimated to result in less than a 5% error in x-ray yields that are taken to be representative of excitation by projectiles of a given incident charge state. This estimate is based on the observed charge-state dependence of x-ray yields (see Sec. IV). At one projectile energy (25.7 MeV), cross sections were measured in a different gas cell described in a previous publication.[20] Gas pressures up to 100 m-Torr were used in this different cell in order to obtain reasonable counting rates. Although yields obtained under these conditions were ~50% smaller than those measured in the other gas cell at lower pressures, the relative trends of the data were not significantly affected. The difficulty in maintaining the gas cell at high pressure without flooding the intermediate pumping region accounts for the discrepancy in cross sections obtained with this configuration, but the similar trends obtained give us confidence that multiple collisions do not significantly influence the experimental results.

III. DATA ANALYSIS

A. X-ray spectra and yields

Sample x-ray spectra taken with the multichannel analyzer are shown in Figs. 1 and 2 for Cl and S beams at the same velocity (10^9 cm/sec) in various targets. Data were taken with two different detectors and the analysis is somewhat different in the two cases. All spectra in Fig. 1 were taken with detector A; those in Fig. 2 were taken with detector B. The low-energy tail of x-ray peaks (mentioned in Sec. II) is particularly evident in Fig. 1(b). This tailing behavior has been studied previously[20] and represents real x-ray events degraded in energy from the full-energy x-ray peak by incomplete charge collection. The contribution of the tail to the full-energy peak is clearly greater for detector A than for detector B.

The resolution of the former detector is somewhat better than the latter in spite of the tailing, and the Cl K x rays were partially resolved into two peaks (see Fig. 1). The low-energy peak (denoted Cl '$K\alpha$') is made up of $K\alpha$ satellites[23] while the higher-energy peak (denoted Cl '$K\beta$') is made up of $K\alpha$ hypersatellites[24] as well as $K\beta$ satellites and hypersatellites. Of interest is the appearance of the '$K\beta$' peak for Cl projectiles with no $3p$ electrons. The results of Woods *et al.*[14]

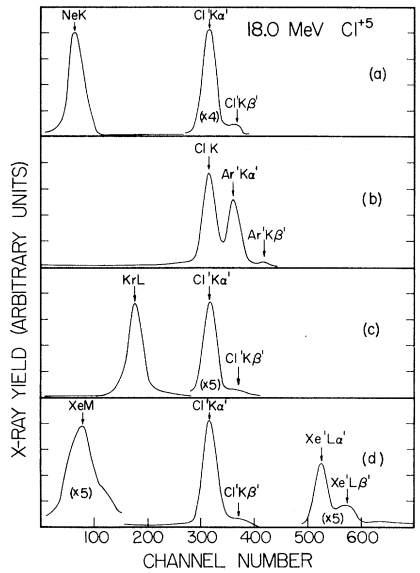

FIG. 1. Typical x-ray spectra for chlorine ions incident on (a) Ne, (b) Ar, (c) Kr, and (d) Xe. The chlorine ions have an energy of 18 MeV and an incident charge state of +5.

give evidence that these '$K\beta$' x rays may be the result of double Cl K-shell ionization. Excitation of Cl $2p$ electrons simultaneous with or previous to Cl K-shell ionization may partially contribute to the '$K\beta$' x-ray production. Another plausible interpretation to account for these transitions requires electron capture to the M shell in the same

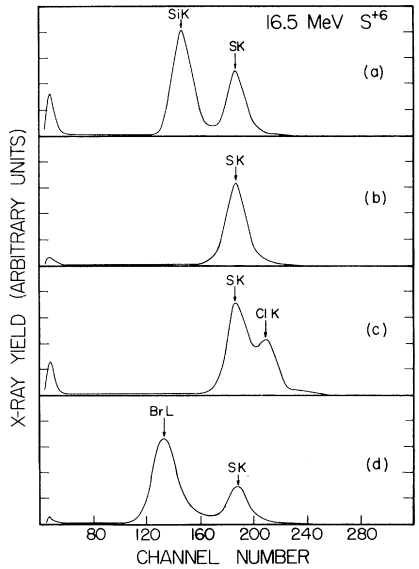

FIG. 2. Typical x-ray spectra for sulfur ions incident on (a) SiH_4, (b) H_2S, (c) HCl, and (d) HBr. The sulfur ions have an energy of 16.5 MeV and an incident charge of +6.

collision in which K-shell vacancies are produced. S'$K\alpha$' and S'$K\beta$' x rays were also observed with detector A; however, for detector B, the resolution was insufficient to separate the two peaks for either Cl or S projectiles.

In Cl-Xe and S-Xe collisions, a broad x-ray peak centered at about 1 keV was observed [see Fig. 1(d)]. This peak, which may be attributed to the filling of Xe M-shell vacancies, may have contributions from $3s$-$4p$, $5p$ and $3p$-$5s$ transitions, which have energies in the range 850 to 1150 eV for the Xe atom. The highest energy XeM x rays reported previously (705 eV) were attributed to a $3d$-$4f$ transition by Fortner *et al.*[25] They also observed the normal $3d$-$4p$ transition at 530 eV. Such low-energy x rays could not be identified in this experiment because the x-ray transmission through the beryllium window decreases rapidly with decreasing photon energy at energies below 900 eV.

X-ray yields for each peak were obtained by integration of the spectra from the multichannel-analyzer output. The peaks, which represent groups of x-ray lines produced in the filling of vacancies of a particular principal shell, were only partially resolved for neighboring atoms with the 200-eV resolution typical of Si(Li) detectors. Since these partially resolved peaks were of comparable magnitude [for example, S and Cl in Fig. 2(c)], separation—for the purposes of integration—at the channel with minimum counts between the peaks introduced only a small error in the x-ray yields. The accuracy of this simple procedure was checked for representative spectra by approximating each x-ray peak by a Gaussian shape with variable centroid and width to fit each spectrum. The peak-fitting routine gives relative yields of the two x-ray peaks with a precision better than that dictated by the inaccuracy inherent in the assumption of a Gaussian peak shape for the complicated x-ray peaks. By comparing the results of the peak integration done analytically and by spectrum separation, the following uncertainties in x-ray yields resulting from the simplifying integration procedure were determined: less than 2% with detector A and 7% with detector B for the partially resolved Cl-Ar, S-Cl, and S-Ar spectra. The uncertainties are only a small contribution to the total experimental errors and justify the simple procedure used.

Peak areas were corrected for a small linear background present in all spectra. Spectra taken with detector A were also corrected for projectile '$K\beta$' peaks that were hidden beneath large peaks [see Fig. 1(b)] and where applicable were corrected for tailing of the x-ray lines due to incomplete charge collection. For detector B, the contribution of the tail to the full energy peak was estimated to be less than 3% in all cases; hence, no tailing corrections were made.

Corrections for projectile '$K\beta$' x rays which were overlapped by the K x-ray peak of the target in nearly symmetric collisions (S-Ar, Cl-Ar) were made in the following way. Cl and S $K\beta/K\alpha$ ratios were obtained for all spectra for which the '$K\beta$' x rays were clearly present (for example, with targets of Ne and Si). The ratios did not vary greatly as a function of projectile energy and charge state and target atomic number. Therefore, the mean value of the $K\beta/K\alpha$ ratio (0.07) was used to make an additive correction to the projectile K x-ray yield and a subtractive correction to the target yield. The uncertainty in x-ray yields introduced by this correction is estimated to be less than 2%. Contributions to the corrected x-ray yields to account for the low-energy tailing in detector A were 10% for S, K, 10 to 20% for ClK and ArK, and 20 to 30% for Xe L. The variations in these contributions were due to changes in detector operating parameters (for example, bias voltage) between experimental runs. Uncertainties in x-ray yields due to the tailing corrections were estimated to be less than 10% for Xe L x rays and less than 5% in all other cases. For some of the data taken with detector A (namely, that of Table I that has been previously reported[15]), no tailing corrections were made. Therefore, it is not unreasonable to expect a relative error of 10 to 20% between these data and that of Tables II and III, for which corrections were made.

B. X-ray production cross sections

The procedures used to extract x-ray-production cross sections from the x-ray yields have been discussed in a previous publication.[20] The geometrical correction factor for x-ray yields was obtained by integrating the solid angle subtended by the detector over the interaction length seen by the detector. Values used for this factor were 0.00175 cm (25.7-MeV Cl), 0.017 cm (Table I), and 0.019 cm (Tables II–IV). Detector efficiencies were calculated as a function of x-ray energy for the absorptive layers of the detectors, and these have been reported previously.[20] Values of efficiency used in this experiment were 0.48 $\pm$ 15% for Br L, 0.52 $\pm$ 15% for Kr L, and 0.55 $\pm$ 15% for SiK, 0.73 $\pm$ 10% for SK, 0.82 $\pm$ 7% for ClK, 0.86 $\pm$ 7% for ArK, and 0.95 $\pm$ 2% for Xe L. For the NeK x rays, for which the calculated efficiency was extremely uncertain (about 80% uncertainty), the efficiency correction was deduced by normalizing the NeK x-ray yield for 52.2-MeV Cl^{+8} on Ne to the NeK x-ray-production cross

TABLE I. Target and projectile x-ray-production cross sections for Cl projectiles of energy E and charge state q incident on He, N_2, Ne, Ar, Kr, and Xe.

		X-ray-production cross section (10^{-22} cm^2)									
E		Target radiation						ClK Projectile Radiation			
(MeV)	q	NeK [b]	ArK	KrL	XeL	He	N_2	Ne	Ar	Kr	Xe
3.0	2	7.0						0.0154			
5.0	3	77	3.22	111	1.33			0.0365	7.88	1.62	21.0
8.0	3	230	7.32	204	7.55		0.0685	0.241	18.4	7.88	74.0
12.6	4	650	14.8	285	18.0	0.181	0.530	2.43	35.8	20.3	127
18.0	5	870	53.5	456	34.2	0.71	2.81	8.37	91.0	54.0	210
25.7[a]	5	590	88.4	664	52.9	2.79	12.2	21.8	135	87	254
35.0	7		195	1330	163				324	239	506
40.0	7	2500	218	1490	149	8.99	68.2	113	358	329	644
45.0	8	4000	278	1840	184	11.1	102	159	406	444	854
52.2	8	4300	312	2110		14.4	155	232	499	627	

[a] These data taken at pressures up to 100 mTorr. Absolute uncertainties may be as high as ±50%.
[b] Absolute uncertainty in this data is estimated at ±50%.

section reported by Burch *et al.*[26] for 50-MeV Cl^{+8} on Ne. The resulting efficiency was 0.025 ± 40%, a reasonable value for the detectors used. This same value was used for all the NeK x-ray yields. A large relative as well as absolute uncertainty in the NeK x-ray production cross sections must be expected, since the detector efficiency is sensitive to possible small shifts in the distribution of NeK x-ray lines (to be discussed in Sec. III C). Efficiency corrections were not made for the XeM x-ray yields owing to the complex structure of the XeM x-ray peak and a lack of data for comparison. For these x rays, values of the normalized x-ray yields (x-ray-production cross section times detector efficiency) are given in Table IV.

Absolute yields determined with detector B were typically 30% higher than corresponding yields obtained with detector A when the solid angles were maximized. The discrepancy is due to differences in detector geometry and shadowing which result from the short detector-to-beam-line distance used. When shadowing effects were minimized by increasing the detector-to-beam-line distance considerably, the yields with the two detectors agreed. However, at these larger distances counting rates were very low for the collisions studied in this experiment and the shortest possible distance was used. Geometrical characteristics for detector A, with the large solid angle, were determined by normalizing to known

TABLE II. Target x-ray-production cross sections for a range of projectile charge states q for Cl and S ions of energy E incident on Ne, SiH_4, H_2S, HCl, Ar, HBr, Kr, and Xe.

			Target x-ray-production cross section (10^{-22} cm^2)							
Z_1	E (MeV)	q	NeK [a]	SiK	SK	ClK	ArK	BrL	KrL	XeL
16	16.5	5	820	193	103[b]	62.9	40.4	394	489	18.4
		6	1000	213	116[b]	73.2	42.9	404	470	19.5
		7	1600	237	130[b]	84.0	50.0	477	510	21.3
		8	2500	310	168[b]	89.4	64.7	460	596	21.7
		9	3500	526	214[b]	133	76.2	485	919	39.0
17	18.0	5	960	172	94.9	69.1[b]	52.9		456	32.5
		6	1000	191	100	80.8[b]	56.2		443	30.0
		7	820	212	122	90.2[b]	63.4		523	40.1
		8	1800	267	147	110[b]	74.1		601	41.8
		9	3400	351	186	147[b]	95.1		711	45.0
		10	5500				128		839	51.6
		11	8800				167		943	55.0
17	30.0	6					120		837	
		11					253		1700	

[a] Absolute uncertainty in these data is estimated at ±50%.
[b] These data obtained by interpolation (see text).

TABLE III. Projectile K x-ray-production cross sections for a range of projectile charge states q for Cl and S ions of energy E incident on Ne, SiH_4, H_2S, HCl, Ar, HBr, Kr, and Xe.

Z_1	E (MeV)	q	Projectile K x-ray-production cross section (10^{-22} cm^2) Ne	SiH_4	H_2S	HCl	Ar	HBr	Kr	Xe
16	16.5	5	18.3	82.3	116[a]	123	128	95.8	128	250
		6	20.7	92.0	131[a]	143	138	97.3	143	286
		7	21.3	98.6	147[a]	167	163	104	155	294
		8	24.7	125	190[a]	184	216	144	174	318
		9	29.3	168	242[a]	263	258	171	223	370
17	18.0	5	8.76	40.6	78.1	77.9[a]	88.4		58.1	176
		6	9.76	45.5	84.8	91.2[a]	96.0		59.0	254
		7	10.2	49.8	95.2	102[a]	109		62.2	222
		8	9.71	60.7	119	123[a]	131		67.0	239
		9	11.9	72.6	156	165[a]	173		81.4	270
		10	14.4				231		91.2	301
		11	17.7				304		102	330
17	30.0	6					205		144	
		11					452		226	

[a] These data obtained by interpolation (see text).

x-ray yields. Results obtained with detector B were normalized to those from detector A. Because of this normalization an uncertainty of about 5% was introduced that applies to the cross sections of Tables II and III and the corresponding normalized yields of Table IV.

No corrections were applied to the projectile x-ray-production cross sections for molecular-gas targets containing hydrogen atoms (SiH_4, H_2S, HCl). However, the small contributions to the projectile cross sections from collisions with these "spectator" hydrogen atoms may be estimated using the following arguments. The Cl K x-ray cross sections for Cl on He, when corrected by the atomic fluorescence yield,[27] compare well with calculations of Coulomb ionization in the plane-wave Born approximation[3] for Cl K-vacancy production in collisions of alpha particles with Cl atoms. For example, the ratio of experimental to theoretical cross sections varies from 0.55 at 0.52 MeV/amu to 0.86 at 1.5 MeV/amu. (The increasing ratio with energy may be attributed to the reduction of increased binding and Coulomb deflection effects.[6]) Given the reasonable comparison, one may estimate the Cl K-shell ionization cross section for Cl on H by using the Z_1^2 scaling law of the Coulomb ionization cross section for Cl on H by dividing the Cl-on-He cross section by 4. At 18-MeV, the Cl K x-ray-production cross section per H atom determined by this procedure is about 0.4×10^{-22} cm^2/atom. Estimated contributions of H atoms to the observed Cl K x-ray-production cross sections in hydride targets at 18 MeV are 4%for SiH_4, 1% for H_2S, and 0.5% for HCl.

For the collisions Cl on HCl and S on H_2S, the target and projectile x rays are indistinguishable [see Fig. 2(b)]. The following procedure was used to estimate separate target and projectile K x-ray-production cross sections in these collisions. For 18-MeV Cl-on-SiH_4, Cl-on-H_2S, and Cl-on-Ar collisions and 16.5-MeV S-on-SiH_4, S-on-HCl,

TABLE IV. Normalized Xe M x-ray yields for Cl and S projectiles of energy E and charge state q. These yields are the product of x-ray-production cross sections times the detector efficiency. The latter correction is not made because the attenuation of the complex Xe M spectrum in the 0.025-mm Be window is not known.

E (MeV)	q	Normalized Xe M x-ray yield (10^{-22} cm^2) $Z_1=17$	$Z_1=16$
5.0	3	11.2	
8.0	3	26.2	
12.6	4	38.9	
18.0	5	64.8	
35.0	7	117	
40.0	7	152	
45.0	8	197	
18.0	5	45.5	
	6	69.6	
	7	60.6	
	8	67.2	
	9	88.8	
	10	111	
	11	135	
16.5	5		52.4
	6		62.4
	7		73.2
	8		84.0
	9		90.0

and S-on-Ar collisions, the ratios of target-to-projectile K x-ray cross sections were formed as a function of incident charge state. Within experimental errors, the ratio of yields for a given collision pair were independent of charge state; therefore, an average of the ratio over charge state was calculated. These ratios were plotted as a function of target atomic number, and ratios for Cl-on-HCl and S-on-H_2S collisions were interpolated. In both cases, a value of approximately 0.90 was found for the ratio target-to-projectile yield, and this was used to separate the total yield into individual target and projectile yields. A ratio of less than unity is not surprising since these collisions are slightly asymmetric due to the ionic state of the projectile. The larger projectile cross section indicated by this procedure may be the result of higher fluorescence yields for the charged projectile than for the neutral atom.

X-ray-production cross sections calculated according to the procedures outlined above are listed in Tables I–III. In Table I, target and projectile cross sections are listed for different values of projectile energy. Target cross sections are given for different charge states at the same energy for Cl and S projectiles in Table II, and the corresponding projectile cross sections are given in Table III. In addition to previously mentioned uncertainties, the cross sections have absolute uncertainties of 10% for manometer calibration and 10% for the geometric normalization factor. Summing in quadrature over all uncertainties yields a total absolute uncertainty of 20 to 25%. Ignoring systematic uncertainties due to manometer calibration, detector efficiency, geometry, and peak integration procedures, the relative uncertainty between cross sections for the same x-ray peak is about 7%. (For NeK x-ray cross sections, the uncertainties are somewhat higher owing to the detector-efficiency correction previously discussed. Absolute uncertainty is estimated at 50% and relative uncertainty at 20%.)

C. Vacancy-production cross sections

If one is to use measurements of x-ray-production cross sections to reach conclusions regarding inner-shell-vacancy production, knowledge of the variation of mean fluorescence yield of the states produced in the collisions is essential. This mean fluorescence yield is a weighted average of the fluorescence yields corresponding to the particular states produced. The weighting factor for each state is the relative population of that state. Since the distribution of final states may depend on such parameters as energy, charge state, and projectile and target atomic number, the mean fluorescence yield is expected to depend on these parameters.

The following procedure has been used to assess the magnitude of fluorescence-yield variations for the x rays observed in this experiment. The ratio of target x-ray-production cross section to projectile x-ray-production cross section has been formed as a function of projectile charge state for 18-MeV Cl ions on targets of SiH_4, H_2S, Ar, Kr, and Xe. The results are shown in Fig. 3. In all cases, the ratios for a particular target are very nearly independent of charge state. This fact is an indication that the mean fluorescence yields of both the target and the projectile do not change substantially for the cases shown. Similar results have been obtained for 16.5-MeV S on SiH_4, HCl, Ar, HBr, Kr, and Xe. For Ne, however, as shown in Fig. 4, the results are much different. The ratio of the NeK x-ray-production cross section to the projectile K x-ray cross section increases rapidly with charge state for both 18-MeV Cl and 16.5-MeV S projectiles. This rise may be attributed to an increasing NeK fluorescence yield similar to the conclusions drawn by Burch *et al.*[26] for 50-MeV Cl on Ne. Some, but not all of this rise, may be due to decreasing detector-window absorption of the NeK x rays as the distribution of these x rays shifts upward in energy with increasing projectile charge state. Similarly, for 18-MeV Cl on Xe, the cross-sec-

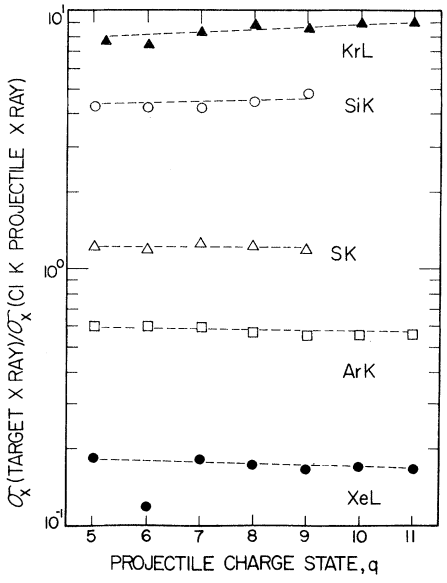

FIG. 3. Target-to-projectile x-ray-production cross-section ratios as a function of projectile charge state q for 18-MeV Cl^{+q} incident on SiH_4, Ar, Kr, Xe, and H_2S. The dashed lines guide the eye through the data for each target.

tion ratios for XeM x rays increase by a little less than a factor of 2 over the range of charge states + 5 to + 11. This increase is attributable to increasing fluorescence yield, vacancy production, or both. The relative importance of these two effects cannot be ascertained from the present results, and clarification requires study of the Auger decay of these collision systems.

With the exception of states that decay by NeK and XeM x rays, the preceding results indicate that the mean fluorescence yields for both target and projectile are independent of charge state in the range studied and the x-ray-production cross sections obtained in this experiment provide a sufficiently accurate means of interpreting the trends of vacancy production. The results of NeK x rays warrant special consideration in discussions of vacancy production, and the XeM cross sections cannot be interpreted with clarity.

One additional observation is worth noting in regard to this discussion. If the mean fluorescence yield is independent of collision parameters (energy, charge state, etc.), then the distribution of final states may be expected to remain the same. Hence, the x-ray energy corresponding to this distribution should be constant. Our spectral observations do indeed show that the centroid energies of the x-ray peaks resulting from deexcitation of a given shell of a given target or projectile are constant within the experimental uncertainty of 10 eV.

To make comparisons with theory, K-vacancy-production cross sections were calculated from the x-ray-production cross sections using values of fluorescence yields taken from the review paper of Bambynek *et al.*[27] Considerable absolute uncertainties are expected in these values because of the high degree of ionization of both target and projectile.

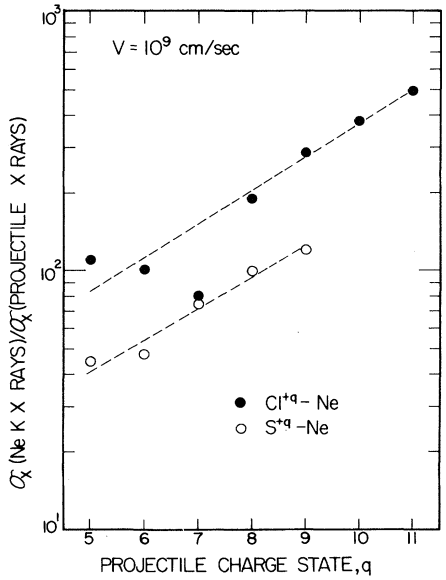

FIG. 4. Target-to-projectile x-ray-production cross-section ratios as a function of projectile charge state q for Cl and S ions incident on Ne at 10^9 cm/sec.

IV. RESULTS AND DISCUSSION

Chlorine projectile K x-ray-production cross sections are plotted in Fig. 5 as a function of target atomic number at four projectile energies. The data at 5.0 and 8.0 MeV and a portion of the data at 18.0 MeV have been previously published.[15] In that publication, the projectile cross sections for the quasisymmetric Cl-Ar collisions are interpreted as being anomalously high with respect to those for the other targets (He, N_2, Ne, Kr, Xe). This interpretation is based on two observations: (i) The nonmonotonic trend of the ClK x-ray cross sections with target atomic number and (ii) the weaker projectile energy dependence of the ClK cross sections for argon targets as compared to the other targets (see Fig. 6). Additional evidence of anomalous behavior in the quasisymmetric region is offered by new data for 18-MeV Cl on HCl and Cl on H_2S, for which the projectile K x-ray-production cross sections are approximately the same as those for Cl on Ar (see Fig. 5).

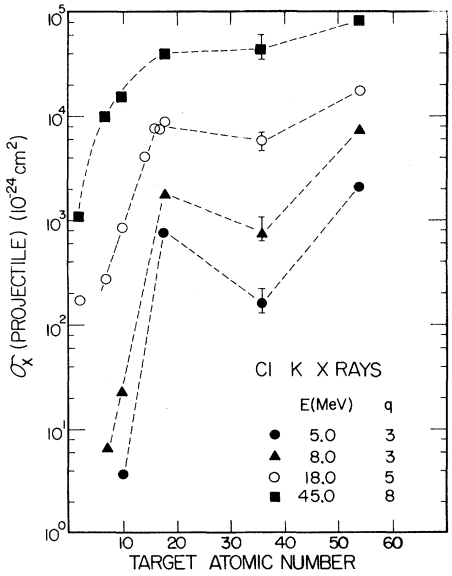

FIG. 5. Projectile K x-ray-production cross section as a function of target atomic number for Cl ions incident on gas targets at four energies. The error bars indicate the typical absolute uncertainty at each energy. The relative uncertainty at each energy is given approximately by the size of the data points. The dashed lines guide the eye through the data at each energy.

Similar results are obtained for projectile K x-ray-production cross sections for 16.5-MeV S ions incident on gaseous targets (see Fig. 7). These cross sections cluster in the region of nearly symmetric collisions ($Z_2 = 16, 17, 18$) and show the nonmonotonic trend with target atomic number that corresponds to an enhanced cross section for symmetric collisions. In addition, there appears to be gross structure in the variation with Z_2 of projectile x-ray cross section for the heavier targets. For example, the already low cross sections for SK x-ray production in Kr is even 30% lower in a target of HBr. The purpose of this work is to investigate the near-symmetric region for Cl and S ions; hence, the details of the gross variation in cross section for $Z_2 \sim 36$ will not be discussed further.

The observation of nonmonotonicity of chlorine projectile cross sections is related to results of Woods *et al.*[14] for ratios of double-to-single Cl K-shell ionization and to results of Cocke *et al.*[28] for the probability of ClK x-ray emission as a function of impact parameter at MeV/amu projectile velocities. In the interpretation of these observations, the x-ray production is assumed to be influenced by mechanisms other than direct Coulomb ionization, for which the perturbing Coulomb potential that induces target (projectile) inner-shell ionization is linear in projectile (target) nuclear charge. An interpretation that is plausible for the quasisymmetric collisions in thick, solid targets has been suggested[13,14] to account for the enhanced vacancy production. This interpretation is based on a transition between the $2p\sigma$ and $2p\pi$ orbitals of the transient molecular system induced by rotational coupling of these orbitals at small internuclear separations. Initial $2p$ vacancies are a prerequisite for the transition to occur, and it has been assumed that these are produced in the projectile by prior collisions in the solid targets. For the thin, gaseous targets used in this experiment, however, the multiple-collision porcess may be inadequate to explain the large cross sections observed in nearly symmetric collisions. When the initial charge state is chosen so that the projectile $2p$ shell is filled [for example, charge states 7 (6) or less for Cl (S) ions], $2p$ vacancies that are required to permit the suggested molecular coupling are not carried into the K-vacancy-producing collisions unless the following conditions hold: (i) the projectile $2p$ excitation cross sections are at least an order of magnitude greater than the single-electron loss cross sections ($\sim 10^{-17}$ cm^2)[19] and (iii) the lifetimes of these excited states are sufficiently long to have small probability of decay throughout the target length. The first condition has not been tested; the second is possible since nanosecond lifetimes of such states have been observed.[29] The probability of

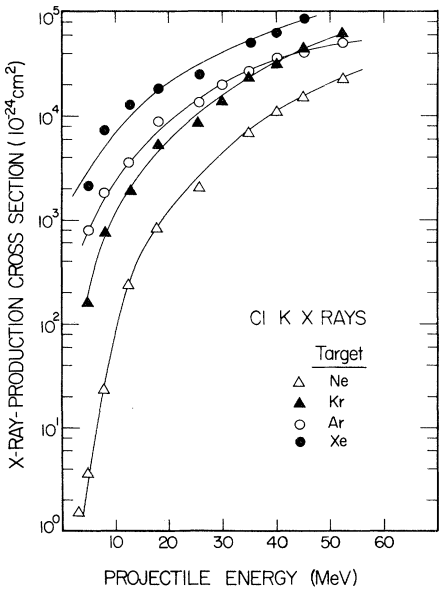

FIG. 6. ClK x-ray-production cross section as a function of projectile energy for Cl ions incident on Ne, Ar, Kr, and Xe. The relative uncertainty in cross sections is approximately the size of the data points. The solid lines guide the eye through the data for each target gas.

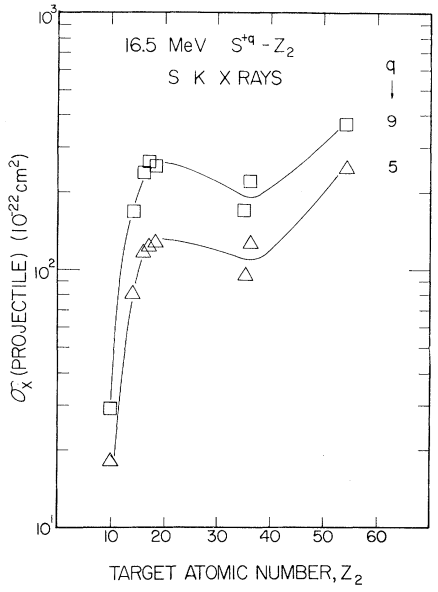

FIG. 7. Projectile K x-ray-production cross sections as a function of target atomic number for 16.5-MeV S ions in charge states +5 and +9 incident on gas targets. The relative uncertainty in cross sections is approximately the size of the data points. The solid lines guide the eye through the data for each charge state.

excitation of projectile $2p$ electrons is an important consideration if the $1s$-vacancy-production mechanisms are enhanced by initial projectile $2p$ vacancies.

In an effort to assess the effect of such vacancies, we have measured x-ray-production cross sections as a function of projectile charge state for Cl and S ions at 10^9 cm/sec incident on the gases Ne, SiH_4, H_2S, HCl, Ar, HBr, Kr, and Xe. The projectile cross sections are plotted in Fig. 8 for Cl ions and Fig. 9 for S ions. For all targets, these cross sections increase with increasing projectile charge state; however, the rate of increase is greater for the quasisymmetric collisions (this includes SiH_4 targets as well as H_2S, HCl, and Ar) than for the asymmetric collisions (targets of Ne, HBr, Kr, and Xe). Similar results are obtained for the target x-ray-production cross sections in quasisymmetric collisions (see Fig. 3) since the ratios of target-to-projectile K x-ray cross sections are approximately constant as a function of projectile charge state. For the asymmetric collisions the target x-ray production cross sections also have the less-pronounced charge-state dependence since the ratios shown in Fig. 3 show only small upward or downward trends with charge state (except for the case of Ne targets, for which the large variation attributed to fluorescence yield was discussed previously).

The fact that the x-ray-production cross sections increase approximately exponentially with charge state could be expected from previous measurements[8,15,30] but have not been explained theoretically. These increases may be the result of a number of factors; among these are reduced screening of the projectile for higher charge states, small changes in fluorescence yields, opening of channels for excitation of projectile K electrons, and multiple processes involving charge exchange and excitation. The important observation of this experiment is that the charge-state dependence is significantly increased for the quasisymmetric collisions as compared to the asymmetric collisions. (For example, in the range $5 \leq q \leq 11$, the Cl K x-ray cross sections increase about a factor of 2 for Cl on Kr and a factor of 3 for Cl on Ar.) These results suggest the increasing importance of $2p\sigma$-$2p\pi$ transitions to K-vacancy production in nearly symmetric collisions as $2p$ electrons are removed from the projectile.

Two considerations are important to make at this point in the discussion: (i) Since the $1s$ level of the lower-Z collision partner becomes the $2p\sigma$ orbital of the transient molecule, the $1s$ electrons of the lighter partner are the only ones that can be excited via the $2p\sigma$-$2p\pi$ transition. Therefore,

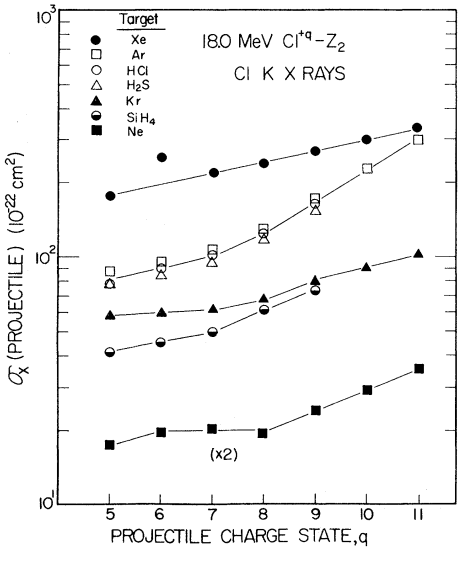

FIG. 8. Projectile K x-ray-production cross section as a function of projectile charge state for 18-MeV Cl ions incident on Ne, SiH_4, H_2S, HCl, Ar, Kr, and Xe. The relative uncertainty in cross sections is approximately the size of the data points. The solid lines guide the eye through the data for each target.

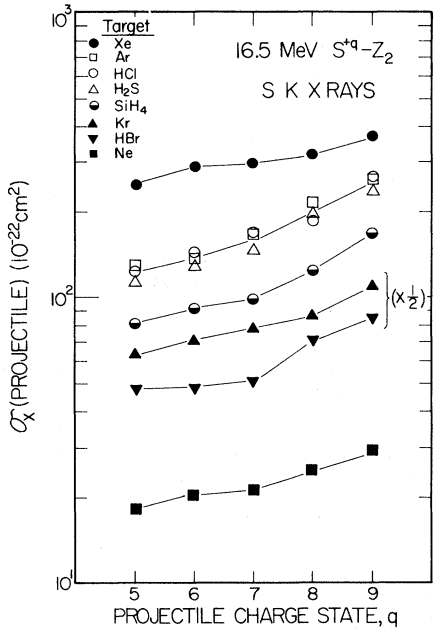

FIG. 9. Projectile K x-ray-production cross section as a function of projectile charge state for 16.5-MeV S ions incident on Ne, SiH_4, H_2S, HCl, Ar, HBr, Kr, and Xe. The relative uncertainty in cross sections is approximately the size of the data points. The solid lines guide the eye through the data for each target.

this transition alone is inadequate to explain the similar magnitudes and trends of *both* target and projectile K x-ray cross sections in nearly symmetric collisions. This point will be discussed later in this section. (ii) The lower-lying $2p$ level of the collision partners becomes the $2p\pi$ orbital of the transient molecule; therefore, vacancies must exist in this level in order for the $2p\sigma$-$2p\pi$ transition to occur. Only the projectile can enter the collision with initial $2p$ vacancies; hence, for $Z_1 < Z_2$, the projectile must be sufficiently highly ionized to depress its $2p$ level below that of the heavier target. Thus, one might expect a discontinuity in the charge-state dependence of the x-ray cross sections at the charge state for which the $2p$ levels of the collision partners swap. (For Cl on Ar, Woods *et al.*[14] estimate that this swapping occurs between $q = +8$ and $+9$.) The smooth trends with charge state seen in our data do not support the speculation that such a discontinuity occurs. This result suggests that other K-vacancy-production processes occur with sufficient magnitude to mask such a break. On the other hand, the lack of a discontinuity may indicate that the prerequisite $2p$ vacancies for $2p\sigma$-$2p\pi$ transitions to occur are formed with high probability in these K-vacancy-producing collisions and, therefore, the charge-state dependence of the cross sections is washed out to some degree even though single-collision conditions prevail.

Further evidence to aid in distinguishing between these possibilities is supplied in Fig. 10. In this figure, calculated cross sections for the $2p\sigma$-$2p\pi$ transition in the symmetric Cl-Cl system are compared with experimental cross sections derived from Cl-on-Ar collisions as a function of projectile energy. The theoretical cross sections have been obtained by scaling the $2p\sigma$-$2p\pi$ cross sections for D^+-D collisions up to $Z = 17$ in a manner suggested by Briggs and Macek.[11] They show that similar scaling for Ne^+-Ne results in good agreement with previous experimental measurements for these collisions. The theoretical curve of Fig. 10 assumes no restriction—other than that dictated by the Pauli principle—on the availability of $2p$ vacancies. If N $2p$ vacancies are initially present, then the theoretical $2p\sigma$-$2p\pi$ cross section must be multiplied by $N/6$ to obtain the K-vacancy-production cross section.[11] Experimental cross sections for comparison to theory are available at only one energy (18 MeV) for the Cl-on-HCl system. However, the energy dependence of total (target plus projectile) K x-ray cross sections for Cl-on-Ar collisions has been measured; and at 18 MeV, the total K x-ray cross section for Cl^{+5} on HCl is close to that for Cl^{+5} on Ar. Therefore, we have used the Cl-on-Ar cross sections, with slight modifications, for the experimental points of Fig. 10. The modification was done as follows: (i) Total K-vacancy-production cross sections were calculated for the Cl-Ar and Cl-HCl collisions using atomic fluorescence yields for the target and projectile.[27] (ii) The ratio of the total K-vacancy-production cross section for 18-MeV Cl^{+5} on HCl to that for 18-MeV Cl^{+5} on Ar was found to be 1.1 and hence the Cl-on-Ar total cross sections at each energy were multiplied by this value to obtain the points plotted in Fig. 10. From the figure, one sees that for no initial $2p$ vacancies, the energy dependence of the experimental cross sections is much steeper than the theoretical result. At the lowest energy, the difference between theoretical and experimental results is nearly a factor of 30. In comparison, for the two cross sections obtained with four initial Cl $2p$ vacancies, the agreement between theoretical and experimental results is good, particularly if the theoretical curve were lowered to account for only four vacancies.

Meyerhof[16] has compared our Cl-on-Ar data for no initial $2p$ vacancies to calculations of H^+-on-H $2p\sigma$ ionization cross sections[31] scaled to Cl-on-Cl collisions. This vacancy-production process is the excitation to the continuum or to levels of high principal quantum number of an electron that

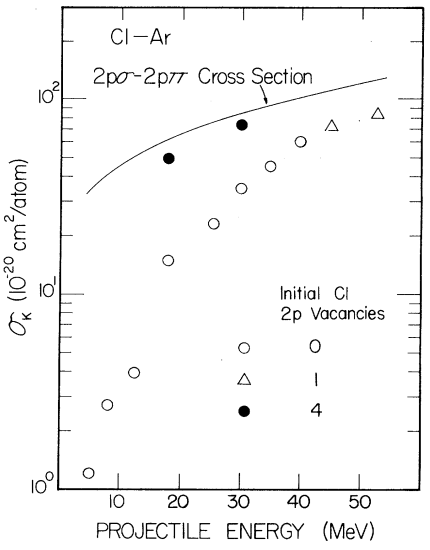

FIG. 10. Total K-vacancy-production cross sections for Cl-Ar collisions as a function of projectile energy for projectiles with 0, 1, and 4 initial $2p$ vacancies. The solid curve is the cross section for $2p\sigma$-$2p\pi$ transition in Cl-Cl collisions calculated from Ref. 11. The relative uncertainty in the data is given approximately by the size of the data points. The absolute uncertainty may be largely due to the systematic uncertainty in the choice of fluorescence yield.

has been promoted along the $2p\sigma$ orbital of the transient molecule formed during the collision. The excitation mechanism is the rotational coupling of the $2p\sigma$ orbital with the vacant high-lying states to which excitation occurs. Meyerhof[16] has demonstrated that the energy dependence as well as absolute magnitude of the calculated cross sections for this process compare well with the experimental results.

These observations suggest the occurrence of two competing K-vacancy-producing mechanisms in the symmetric collisions. For projectiles with no initial $2p$ vacancies, a one-step mechanism such as $2p\sigma$ ionization may dominate the K-vacancy production. Conversely, for projectiles with large numbers of initial $2p$ vacancies, the one-step $2p\sigma$-$2p\pi$ transition may dominate. There is no evidence in this work for the occurrence of the two-step mechanism of $2p$-vacancy production and $2p\sigma$-$2p\pi$ transitions in single collisions. However, the experimental data do not necessarily exclude this mechanism. That is, the energy dependence of the $2p\sigma$-$2p\pi$ cross section will be modulated by the energy dependence of $2p$-vacancy production in this two-step process. If the latter dependence is strong, it may result in an energy dependence of the K-vacancy-production cross sections more nearly resembling that experimentally observed for no initial $2p$ vacancies. Measurements of Cl $2p$-vacancy-production cross sections may be necessary to test these speculations. Additional measurements of the energy dependence of K-vacancy-production cross sections in symmetric collisions for projectiles with given numbers of initial $2p$ vacancies are also needed to examine the contribution of $2p\sigma$-$2p\pi$ transitions to the vacancy production.

Neither the $2p\sigma$-$2p\pi$ transition nor the $2p\sigma$ ionization can account for the similarities between target and projectile K x-ray production in the quasi-symmetric collisions. Not only do these cross sections show nearly identical trends with projectile charge state (see Fig. 3), but they also have similar magnitudes. Transitions beginning on the $2p\sigma$ orbital may have large cross sections for the lower-Z collision partner only; the $1s$ electrons of the higher-Z partner are forced downward in energy along the $1s$ orbital, and a low vacancy-production cross section would be expected. Enhancements of K x-ray-production cross sections for the higher-Z partner in nearly symmetric collisions have previously been observed,[13] and Meyerhof[18] has proposed a K-vacancy transfer mechanism to account for the phenomenon. According to this mechanism, vacancies produced in the $2p\sigma$ orbital on the incoming part of the trajectory can be transferred by radial coupling to the $1s$ level of the higher-Z collision partner on the outgoing part of the trajectory. The transfer probability given by Meyerhof is $W=(1+e^{2|x|})^{-1}$, where $x=\pi(I_1-I_2)/(8mI)^{1/2}v$. [$I_1$ and I_2 are the K binding energies of projectile and target, m is the electron mass, I is the $2p\sigma$ ionization energy and is approximated by $I^{1/2}=\frac{1}{2}(I_1^{1/2}+I_2^{1/2})$, and v is the projectile velocity.] Meyerhof[18] has shown this theoretical result to give reasonable agreement with experimental measurements for Ni, Br, and I projectiles incident on solid targets.

We have compared the theoretical transfer probability given above to our experimental measurements of K x-ray-production cross sections. The results are shown in Fig. 11. The experimental points were obtained by calculating vacancy-production cross sections from the x-ray cross sections and plotting the ratios $\sigma_K(H)/[\sigma_K(H)+\sigma_K(L)]$ versus x. (The notation of Meyerhof has been used: σ_K is the K-vacancy-production cross section; H refers to the higher-Z partner, L to the lower-Z partner.) If the K-vacancy transfer mechanism does account for the experimental results, then this cross-section should be W The plotted points are for targets of SiH_4, H_2S, HCl, and Ar with projectiles of Cl and S in the lowest incident charge state used at each energy. Agreement between theory and experiment is within the relative error in most cases. Ratios for Cl on Ne are not shown in the figure, but these range from 0.0001 to 0.03 when a NeK fluorescence yield of 0.05 is assumed.[26] Corresponding theoretical values of

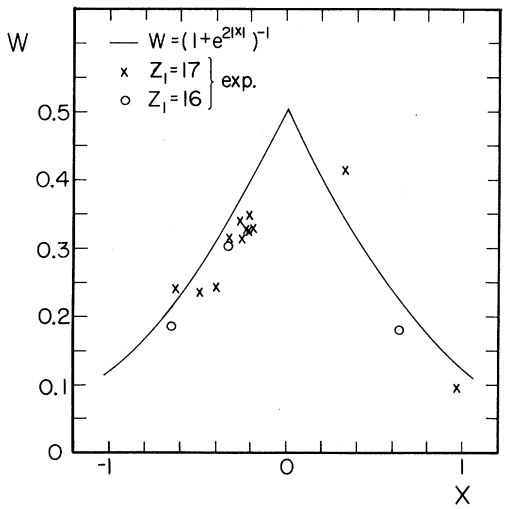

FIG. 11. Probability W of K-vacancy transfer between collision partners as a function of the parameter x described in the text. The solid line is the theoretical result following Ref. 18.

W range from 0.0002 to 0.07, about a factor of 2 in excess of the rather uncertain experimental results. This is considered good agreement and is supportive of the vacancy-sharing process.

In nearly all cases, the experimental cross-section ratios are smaller than the theoretical values. This result is perhaps due to contributions of Coulomb ionization to the vacancy production predominantly in the lower-Z collision partner. In general, agreement between theory and experiment is evidence for the importance of a vacancy transfer process.

V. SUMMARY

X-ray-production cross sections of both target and projectile were measured in collisions of 3.0–52.2-MeV Cl ions with a variety of thin, gas targets from He to Xe. The dependence of these cross sections on incident projectile charge state was measured for both Cl and S projectiles at one velocity (10^9 cm/sec). The dependence of the projectile K x-ray-production cross sections on target atomic number Z_2 is nonmonotonic—anomalously large cross sections being observed in the region of nearly symmetric collisions ($Z_2 \sim 17$). For Cl-on-Ar collisions, the ClK x-ray cross sections exhibit a weaker dependence on projectile energy than for asymmetric collisions such as Cl on Kr; hence, the dependence of the ClK cross sections on Z_2 approaches (and eventually reaches) monotonicity with increasing projectile energy. These observations indicate that the dominant K-vacancy-production processes at these projectile velocities (0.1–1.5 MeV/amu) are different for quasisymmetric collisions than for asymmetric collisions. Processes associated with the formation of a transient molecule may be largely responsible for K-vacancy production for the former.

The incident-charge-state dependence of x-ray-production cross sections also points to differences between symmetric and asymmetric collisions. This dependence is significantly greater for the former than for the latter in nearly all cases. (An exception is the NeK cross section which increases very rapidly with charge state, as a result of the increasing NeK fluorescence yield). The enhanced charge-state dependence of x-ray cross sections for the nearly symmetric collisions suggests the increasing importance of $2p\sigma$-$2p\pi$ transitions in K-vacancy production as the number of initial projectile $2p$ vacancies increases. For Cl projectiles with no initial $2p$ vacancies, however, the energy dependence of total K-vacancy-production cross sections in Cl-on-Ar collisions is much stronger than theoretical results for the $2p\sigma$-$2p\pi$ cross section. For such cases, a different K-vacancy-production mechanism may be dominant; Meyerhof[16] has suggested that this mechanism is the excitation of $2p\sigma$ electrons, to high n, or continuum states.

For the collision partner of higher atomic number in the nearly symmetric collisions, the transitions in the preceding discussion cannot directly contribute to K-vacancy production. However, the cross sections for the higher-Z partner are observed to be very similar to the lower-Z partner in magnitude and charge-state dependence. Meyerhof[18] has proposed that a K-vacancy transfer mechansim may explain such similarities. Comparison of the data with his calculations of the probability for transfer of a K vacancy from the lower- to the higher-Z collision partner indicate that this mechanism may indeed be operative in the collisions studied.

Continued systematic investigation of these collisions is necessary. In particular, we suggest that the following experiments are of importance in the study of the vacancy-production mechanisms: (i) measurements of the energy dependence of total vacancy-production cross sections for projectiles with large numbers of initial $2p$ vacancies in order to determine the importance of $2p\sigma$-$2p\pi$ transitions, and (ii) additional charting of the Z_2 dependence of cross sections by the use of thin, transmission targets available in gaseous phase as a means of studying the mechanisms of K-vacancy production for $Z_2/Z_1 > 1$.

---

*Work partially supported by the U.S. Atomic Energy Commission under Contract No. AT(11-1)-2130.

†This work fulfilled the thesis requirements for the Doctor of Philosophy degree at Kansas State University, 1974.

‡Present address: Cyclotron Institute, Texas A & M University, College Station, Tex. 77843.

§Present address: Fermi National Accelerator Laboratory, P. O. Box 500, Batavia, Ill. 60510.

[1] J. D. Garcia, R. J. Fortner, and T. M. Kavanagh, Rev. Mod. Phys. 45, 111 (1973).

[2] A good experimental as well as theoretical survey is given in M. Barat and W. Lichten, Phys. Rev. A 6, 211 (1972).

[3] E. Merzbacher and H. W. Lewis, in *Handbuch der Physik*, edited by S. Flugge (Springer, Berlin, 1958), Vol. 34, p. 166; G. S. Khandelwal, B. H. Choi, and E. Merzbacher, At. Data 1, 103 (1969).

[4]J. D. Garcia, Phys. Rev. A 1, 280 (1970).
[5]U. Fano and W. Lichten, Phys. Rev. Lett. 14, 627 (1965); W. Lichten, Phys. Rev. 164, 131 (1967).
[6]G. Basbas, W. Brandt, and R. Laubert, Phys. Rev. A 7, 983 (1973).
[7]James R. Macdonald, Patrick Richard, C. L. Cocke, Matt Brown, and Ivan A. Sellin, Phys. Rev. Lett. 31, 684 (1973); S. J. Czuchlewski, M. D. Brown, J. R. Macdonald, L. M. Winters, R. Laubert, J. R. Mowat, and I. A. Sellin, Bull. Am. Phys. Soc. 19, 590 (1974); M. D. Brown, L. D. Ellsworth, J. A. Guffey, T. Chiao, E. W. Pettus, L. M. Winters, and J. R. Macdonald, Phys. Rev. A 10, 1255 (1974).
[8]Loren M. Winters, James R. Macdonald, Matt D. Brown, Tang Chiao, Louis D. Ellsworth, and E. W. Pettus, Phys. Rev. A 8, 1835 (1973).
[9]A. M. Halpern and J. Law, Phys. Rev. Lett. 31, 4 (1973); J. H. McGuire, Phys. Rev. A 8, 2760 (1973).
[10]N. Cue, V. Dutkiewicz, P. Sen, and H. Bakhru, Phys. Rev. Lett. 32, 1155 (1974).
[11]J. S. Briggs and J. Macek, J. Phys. B 5, 579 (1972); 6, 982 (1973).
[12]F. W. Saris and D. J. Biermann, Phys. Lett. A 35, 199 (1971).
[13]H. Kubo, F. C. Jundt, and K. H. Purser, Phys. Rev. Lett. 31, 674 (1973).
[14]C. W. Woods, F. Hopkins, R. L. Kauffman, D. O. Elliot, K. A. Jamison, and P. Richard, Phys. Rev. Lett. 31, 1 (1973).
[15]Loren Winters, James R. Macdonald, Matt D. Brown, Tang Chiao, Louis D. Ellsworth, and E. W. Pettus, Phys. Rev. Lett. 31, 1344 (1973).
[16]T. K. Saylor and W. E. Meyerhof, Bull. Am. Phys. Soc. 19, 592 (1974); W. E. Meyerhof, Phys. Rev. A 10, 1005 (1974).
[17]Loren Winters, James R. Macdonald, M. D. Brown, L. D. Ellsworth, Tang Chiao, and E. W. Pettus, Bull. Am. Phys. Soc. 19, 89 (1974).
[18]W. E. Meyerhof, Phys. Rev. Lett. 31, 1341 (1973).
[19]E. Horsdal Pedersen, M. D. Brown, S. Czuchlewski, L. D. Ellsworth, J. A. Guffey, J. R. Macdonald, and L. M. Winters, Bull. Am. Phys. Soc. 19, 495 (1974).
[20]Loren M. Winters, James R. Macdonald, Matt D. Brown, Louis D. Ellsworth, and Tang Chiao, Phys. Rev. A 7, 1276 (1973).
[21]Ortec, Inc., Oak Ridge, Tenn.
[22]Erik Horsdal Pedersen, Stephen J. Czuchlewski, Matt D. Brown, Louis D. Ellsworth, and James R. Macdonald (unpublished).
[23]Patrick Richard, I. L. Morgan, T. Furuta, and D. Burch, Phys. Rev. Lett. 23, 1009 (1969); D. Burch and Patrick Richard, Phys. Rev. Lett. 25, 983 (1970).
[24]P. Richard, W. Hodge, and C. F. Moore, Phys. Rev. Lett. 29, 393 (1972).
[25]R. J. Fortner, R. C. Der, and T. M. Kavanagh, Phys. Lett. A 37, 259 (1971).
[26]D. Burch, N. Stolterfoht, D. Schneider, H. Wieman, and J. S. Risley, Phys. Rev. Lett. 32, 1151 (1974).
[27]Fluorescence yields were selected from a table of "most-reliable" values in W. Bambynek, B. Crasemann, R. W. Fink, H. U. Freund, H. Mark, C. D. Swift, R. E. Price, and P. V. Rao, Rev. Mod. Phys. 44, 716 (1972). Values used were 0.043 for SiK, 0.082 for SK, 0.0955 for ClK, and 0.122 for Ar K.
[28]C. L. Cocke, R. Randall, and B. Curnutte, in *Proceedings of the Eighth International Conference on the Physics of Electronic and Atomic Collisions, Belgrade, Yugoslavia, 1973*, edited by B. C. Cobic and M. V. Kurepa (Institute of Physics, Beograd, Yugoslavia, 1973), p. 714; R. Randall (private communication).
[29]D. J. Pegg, I. A. Sellin, P. M. Griffin, and Winthrop W. Smith, Phys. Rev. Lett. 28, 1615 (1972); D. J. Pegg, I. A. Sellin, R. Peterson, J. R. Mowat, W. W. Smith, M. D. Brown, and J. R. Macdonald, Phys. Rev. A 8, 1350 (1973).
[30]J. R. Mowat, I. A. Sellin, D. J. Pegg, R. S. Peterson, M. D. Brown, and J. R. Macdonald, Phys. Rev. Lett. 30, 1289 (1973); J. R. Mowat, I. A. Sellin, P. M. Griffin, D. J. Pegg, and R. S. Peterson, Phys. Rev. A 9, 644 (1974).
[31]V. SethuRaman, W. R. Thorson, and C. F. Lebeda, Phys. Rev. A 8, 1316 (1973).